Molecular Biology of the Cell
Vol. 9, 685–699, March 1998

Apiconuclear Organization of Microtubules Does Not Specify Protein Delivery from the Trans-Golgi Network to Different Membrane Domains in Polarized Epithelial Cells

Kent K. Grindstaff,* Robert L. Bacallao,† and W. James Nelson*‡

*Department of Molecular and Cellular Physiology, Stanford University School of Medicine, Stanford, California 94305; and †Division of Nephrology, Indiana University School of Medicine, Indianapolis, Indiana 46236

Submitted September 18, 1997; Accepted December 5, 1997
Monitoring Editor: Peter Walter

In nonpolarized epithelial cells, microtubules originate from a broad perinuclear region coincident with the distribution of the Golgi complex and extend outward to the cell periphery (perinuclear [PN] organization). During development of epithelial cell polarity, microtubules reorganize to form long cortical filaments parallel to the lateral membrane, a meshwork of randomly oriented short filaments beneath the apical membrane, and short filaments at the base of the cell; the Golgi becomes localized above the nucleus in the subapical membrane cytoplasm (apiconuclear [AN] organization). The AN-type organization of microtubules is thought to be specialized in polarized epithelial cells to facilitate vesicle trafficking between the trans-Golgi Network (TGN) and the plasma membrane. We describe two clones of MDCK cells, which have different microtubule distributions: clone II/G cells, which gradually reorganize a PN-type distribution of microtubules and the Golgi complex to an AN-type during development of polarity, and clone II/J cells which maintain a PN-type organization. Both cell clones, however, exhibit identical steady-state polarity of apical and basolateral proteins. During development of cell surface polarity, both clones rapidly establish direct targeting pathways for newly synthesized gp80 and gp135/170, and E-cadherin between the TGN and apical and basolateral membrane, respectively; this occurs before development of the AN-type microtubule/Golgi organization in clone II/G cells. Exposure of both clone II/G and II/J cells to low temperature and nocodazole disrupts >99% of microtubules, resulting in: 1) 25–50% decrease in delivery of newly synthesized gp135/170 and E-cadherin to the apical and basolateral membrane, respectively, in both clone II/G and II/J cells, but with little or no missorting to the opposite membrane domain during all stages of polarity development; 2) ~40% decrease in delivery of newly synthesized gp80 to the apical membrane with significant missorting to the basolateral membrane in newly established cultures of clone II/G and II/J cells; and 3) variable and nonspecific delivery of newly synthesized gp80 to both membrane domains in fully polarized cultures. These results define several classes of proteins that differ in their dependence on intact microtubules for efficient and specific targeting between the Golgi and plasma membrane domains.

INTRODUCTION

The cell surface distribution of membrane proteins in fibroblasts and polarized epithelial cells is distinctly

‡ To whom correspondence should be addressed: Department of Molecular and Cellular Physiology, Stanford University School of Medicine, Beckman Center, B121, Stanford, CA 94305-5426.

different. In general, membrane proteins in fibroblasts are randomly distributed except for specialized cell adhesion complexes that are restricted to the cell–extracellular matrix interface. In polarized epithelial cells, proteins are restricted to discrete membrane domains, termed apical and basolateral. Differences in protein distributions in fibroblasts and epithelial cells are related to specific cellular functions including cell migration and vectorial ion and solute transport, respectively.

Attempts to elucidate mechanisms that establish and maintain cell surface distributions of membrane proteins in polarized epithelial cells have revealed the complex nature of these processes. Early studies in simple epithelia showed that apical and basolateral membrane proteins are sorted into separate transport vesicles in the trans-Golgi Network (TGN) and then delivered to the appropriate membrane domain (Rodriguez-Boulan and Nelson, 1989; Wandinger-Ness *et al.*, 1990). Thus, it was proposed that protein sorting in the TGN is the basis for establishing and maintaining cell surface polarity in epithelial cells. Subsequently, signals for sorting basolateral membrane proteins in the TGN have been identified, although less is known about signals for sorting apical proteins (Matter and Mellman, 1994). Recently, however, Musch *et al.* (1996) and Yoshimori *et al.* (1996) found that marker proteins of epithelial apical and basolateral membranes are sorted into separate vesicles in the TGN of fibroblasts, although these proteins become randomly distributed after delivery to the plasma membrane. These results show that sorting of apical and basolateral membrane proteins in the TGN is not specific to polarized epithelial cells, and that other cellular processes must be required to establish and maintain the asymmetric distribution of plasma membrane proteins characteristic of polarized epithelial cells: targeting of transport vesicles along the cytoskeleton, specific docking of transport vesicles at the correct membrane domain, and resorting or retention of proteins in a specific membrane domain.

The cytoskeleton has been the focus of studies to identify mechanisms involved in vesicle trafficking to, and membrane protein retention at, specific membrane domains. In polarized epithelial cells, the actin cytoskeleton is distributed in a ring around the apex of the lateral membrane at the site of the adherens cell–cell adhesion junction, and along the lateral and basal membranes; in cells that form a brush border (e.g., enterocytes), actin filaments also form the core of individual microvilli (Nelson, 1991; Mays *et al.*, 1994). Disruption of the actin cytoskeleton with cytochalasin appears to have little affect on vesicle trafficking to either the apical or basolateral membrane domain (Salas *et al.*, 1986; Parczyk *et al.*, 1989; Ojakian and Schwimmer, 1992). However, it is noteworthy that myosin is present on purified, post-TGN transport vesicles, indicating that the actin cytoskeleton is involved in vesicle trafficking (Fath and Burgess, 1993). In addition, the actin-based membrane cytoskeleton is required to retain Na/K-ATPase in the basolateral membrane (Hammerton *et al.*, 1991).

Microtubule organization in fully differentiated epithelial cells comprises an apical web of filaments, cortical filaments organized along the apical–basal axis of the cells, and short filaments at the base of the cell (Bacallao *et al.*, 1989; van Zeijl and Matlin, 1990; Gilbert *et al.*, 1991); we term this microtubule organization, apiconuclear (AN)-type, to contrast it with the organization of microtubules in nonpolarized epithelial cells and fibroblasts in which the microtubules are organized from a broad perinuclear region (PN-type) (Bacallao *et al.*, 1989). Previous studies have shown that vesicle transport between the TGN and apical membrane is affected after disruption of microtubules with colchicine or nocodazole, whereas transport to the basolateral plasma membrane is not (Rindler *et al.*, 1987; Achler *et al.*, 1989; Eilers *et al.*, 1989; Matter *et al.*, 1990; van Zeijl and Matlin, 1990). These results were derived from the analysis of protein trafficking in fully polarized epithelial cells, which, when examined, possessed an AN-type microtubule organization before treatment with microtubule-disrupting drugs (van Zeijl and Matlin, 1990; Gilbert *et al.*, 1991). It has been suggested that an AN-type microtubule organization and the coincident relocalization of the Golgi complex to apical region of the cell facilitates efficient delivery of proteins from the TGN to the apical membrane (van Zeijl and Matlin, 1990). However, basolateral transport vesicles bind to microtubules in vitro (Van der Sluijs *et al.*, 1990), and delivery of marker proteins to the basolateral membrane appears to require microtubule motor proteins (Lafont *et al.*, 1994).

We have reassessed the role of microtubules and their specific distribution in protein trafficking. We have used two clones of MDCK cells: clone II/G cells reorganize microtubules and the Golgi complex from a PN-type to AN-type distribution during development of polarity, whereas clone II/J cells maintain a PN-type organization. We show during development of polarity that delivery of both endogenous apical and basolateral marker proteins is efficient and specific before microtubule reorganization from a PN- to AN-type. Furthermore, we find that the efficiency of delivery of both apical and basolateral proteins is decreased upon microtubule disruption. These results show that while microtubules are required for efficient delivery of both apical and basolateral proteins, an AN-type distribution of microtubules and the Golgi complex is not critical for the appropriate targeting of several classes of plasma membrane proteins to the cell surface.

MATERIALS AND METHODS

Cells and Tissue Culture Methodology

Madin-Darby canine kidney (MDCK) clone II/G cells were obtained from the laboratory of Gerrit van Meer and isolated as previously described (Gaush *et al.*, 1966; Louvard, 1980); clone II/J cells were independently isolated in the Nelson laboratory (Nelson and Veshnock, 1986) from a single cell clone from a stock of MDCK cells obtained from The American Type Culture Collection (Gaithersburg, MD). Based upon the transepithelial electrical resistance [200–300 Ω/cm^2], both clone II/G and II/J cells are type II MDCK cells and are indistinguishable with respect to the steady-state localization of Na/K-ATPase, E-cadherin, ankyrin, fodrin, and gp135/170, as assayed by immunofluoresence and cell surface biotinylation (Wollner *et al.*, 1992; Mays *et al.*, 1995a, 1995b).

Cells were maintained in DMEM supplemented with 10% fetal bovine serum (FBS), penicillin, streptomycin, and kanamycin (DMEM/FBS) as previously described (Nelson and Veshnock, 1986). Cells were routinely passaged at low density on tissue culture dishes before plating at confluent density on Transwell 0.45-μm polycarbonate filters (Costar, Cambridge, MA) coated with type I rat tail collagen (Hammerton *et al.*, 1991; Siemers *et al.*, 1993). Cells maintained in culture as confluent monolayers for extended periods of time were refed daily. Low-passage replicates of the clones were propagated for 4–6 wk, and then discarded.

To generate a confluent monolayer of 'contact-naive' cells (Nelson and Veshnock, 1987), cells were maintained at low density (2×10^6 cells/150-mm diameter dish) and passaged on consecutive days. After treatment with trypsin, cells were centrifuged at $1000 \times g$ for 5 min and resuspended in DMEM containing 5 μM Ca^{2+}, supplemented with 10% FBS that had been exhaustively dialyzed against phosphate-buffered saline (PBS) (without Ca^{2+}). Approximately 2×10^6 cells in 2 ml of medium were added to a 2.4-cm^2 Transwell filter coated with type I collagen; 2.5 ml of medium were added to the outside (basolateral) compartment of the filter. After 3 h at 37°C, at which time greater than 95% of the cells had attached to the filter, the medium was replaced with DMEM/FBS containing 1.8 mM Ca^{2+} to induce synchronous cell–cell contacts across the monolayer (Hammerton *et al.*, 1991; Siemers *et al.*, 1993); this modification from a previous protocol (Nelson and Veshnock, 1987) minimizes the time the cells are exposed to low Ca^{2+} in the medium. After the switch to normal calcium-containing medium, the cells were the maintained in culture for up to 120 h as described in the text.

Immunofluoresence Specimen Preparation and Imaging

The fixation and staining method used for examination of the microtubule organization was performed essentially as previously described (Bacallao *et al.*, 1989). At the indicated times after the induction of cell–cell contacts, cells were fixed with 0.5% glutaraldehyde in 100 mM K-piperazine-*N,N'*-bis(2-ethanesulfonic acid) (PIPES), pH 6.9, 4 mM $MgCl_2$, 2 mM EGTA containing 0.1% Triton X-100. The fixation reaction was quenched by treating the sample with 1 mg/ml $NaBH_4$ dissolved in PBS, pH 8.0. After several washes with PBS, the samples were incubated with monoclonal antibodies specific for α- and β-tubulin (Amersham, Arlington Heights, IL). Excess antibody was washed off with PBS containing 0.1% Triton X-100, and samples were incubated with rhodamine-conjugated donkey anti-mouse immunoglobulin G (Jackson ImmunoResearch, West Grove, PA). Excess secondary antibody was washed off with PBS containing 0.1% Triton X-100, and the samples were postfixed with 2% paraformaldehyde dissolved in PBS for 30 min at room temperature. The samples were mounted in PBS containing 50% glycerol and 100 mg/ml 1,4-diazabicyclo (2.2.2) octane (Sigma, St. Louis, MO).

Samples prepared for examination of the Golgi complex were fixed with 2% paraformaldehyde dissolved in PBS for 10 min at room temperature. The fixation reaction was quenched with 50 mM NH_4Cl dissolved in PBS for 30 min at room temperature. Samples were incubated in PBS containing 1% SDS for 1 min. Samples were extensively washed in PBS containing 0.1% Triton X-100 and then incubated with anti-β cop antibody (clone M3A5) (Sigma). Excess antibody was washed off with PBS containing 0.1% Triton X-100, and samples were labeled with Bodipy-conjugated donkey anti-mouse immunoglobulin G (Jackson ImmunoResearch). Excess secondary antibody was washed off with PBS containing 0.1% Triton X-100. The samples were mounted in PBS containing 50% glycerol, 100 mg/ml 1,4-diazabicyclo (2.2.2) octane, and 1 μg/ml of the nucleic acid stain TO-PRO-3 (Molecular Probes, Eugene, OR).

The samples were examined with a Bio-Rad MRC 1024 confocal microscope (Bio-Rad, Richmond, CA) mounted on a Nikon Diaphot 200 inverted microscope (Fryer Scientific Instruments, Huntley, IL) equipped with a He-Ar and Kr-Ar laser. Serial images were collected with a 100× oil immersion lens (numerical aperature 1.4) with a z step of 0.2 μm. Stereo pair images were produced by MetaMorph image-processing program (Universal Imaging, West Chester, PA) on a Micron Millennia computer (Micron Electronics, Nampa, ID). The processed images were adjusted to optimize the contrast and brightness of the images.

Metabolic Labeling

Cell cultures were initially established in DMEM supplemented with 10% FBS as described above. Cells were preincubated in DMEM/FBS in the absence of methionine/cysteine (DMEM/FBS, −met, −cys) for 60 min, and then in DMEM/FBS, −met, −cys containing 250 μCi [^{35}S]methionine/cysteine (Amersham, Arlington Heights, IL) for 1 h at 37°C. Cells were rinsed twice in prewarmed DMEM/FBS, and then incubated in that medium for 5 min, after which time an aliquot was removed from both the apical and basolateral compartments to access gp80 secretion. Filters were then subjected to domain-specific biotinylation as described below.

Domain-specific Biotinylation and Immunoprecipitation

After the metabolic labeling period described above, confluent monolayers of MDCK cells on Costar Transwell polycarbonate filters were washed twice in ice-cold Ringer's saline (154 mM NaCl, 1.8 mM Ca^{2+}, 7.2 mM KCl, 10 mM HEPES, pH 7.4). NHS-SS-Biotin, 300 μg/ml (Pierce Chemical, Rockford, IL), prepared immediately before use in Ringer's saline, was added to either the apical (400 μl) or basolateral (800 μl) compartment of the filter, and the cells were incubated for 30 min at 4°C with constant rocking; Ringer's saline was added to the opposite compartment. The biotinylation reaction was quenched by washing cells in five changes of Tris-saline (120 mM NaCl, 10 mM Tris, pH 7.4) at 4°C or, for microtubule/control samples, two times with microtubule stabilization buffer (0.1 mM PIPES, pH 6.75, 1 mM $MgSO_4$, 1 mM EDTA, 2 M glycerol) at 37°C (van Zeijl and Matlin, 1990). Duplicate filters, which were mock labeled with [^{35}S]methionine/cysteine and biotin (microtubule/control samples), were used to access the presence of functional tight junctions across the monolayer by measuring the diffusion of [^{3}H]inulin (DuPont New England Nuclear, Boston, MA) from the apical to the basolateral compartment during the incubation with biotinylated cross-linking reagent. Only filters that inhibited diffusion of >98% of tracer were used further.

Cell Extraction and Immunoprecipitation

Cells were extracted in radioimmunoprecipitation assay (RIPA) buffer (150 mM NaCl, 10 mM $NaPO_4$, pH 7.0, 0.1% SDS, 1% NP-40, 1% deoxycholate) for 30 min at 4°C (Hinck *et al.*, 1994), or microtubule extraction buffer (0.1 mM PIPES, pH 6.75, 1 mM $MgSO_4$, 1 mM EDTA, 2 M glycerol, 0.1% (wt/vol) Triton X-100) for 20 min at 37°C (van Zeijl and Matlin, 1990). An aliquot from each metabolically labeled sample was removed and precipitated with 10% trichloro-

acetic acid to normalize samples with respect to [^{35}S]methionine/cysteine incorporation. Cell extracts isolated in RIPA buffer (350 μl) were precleared with 5 μl of preimmune serum and 60 μl *Staphylococcus aureus* cells (Pansorbin; Calbiochem Novabiochem, La Jolla, CA) for 60 min at 4°C. At the same time, primary antibody, 15 μl of cadherin antiserum (Marrs *et al.*, 1993), or 40 μl of gp135/170 monoclonal antibody (a gift from Dr. G. Ojakian, SUNY, Brooklyn, NY), was added to Protein A Sepharose (PAS) beads (Pharmacia Biotech, Piscataway, NJ) for 60 min at 4°C. For gp135/170 monoclonal antibody, rabbit anti-mouse secondary antiserum (Dako, Carpinteria, CA) was prebound to PAS beads for 1 h at 4°C before incubation with mouse monoclonal antibodies. Preabsorbed antibody–PAS complexes were added to the precleared extracts and incubated for 120 min at 4°C. Immunoprecipitates were washed under stringent conditions, as described previously (Hinck *et al.*, 1994). Antibody–antigen complexes were dissociated and biotinylated proteins were reprecipitated with avidin-agarose (Pierce Chemical) and washed under stringent conditions, as described previously (Hammerton *et al.*, 1991; Siemers *et al.*, 1993). Cell extracts isolated under microtubule-stabilizing conditions were centrifuged at 20,000 $\times$ *g* and separated into soluble and insoluble fractions. Insoluble fractions were then solubilized in microtubule solubilization buffer (25 mM Tris, pH 7.4, 0.4 M NaCl, 0.5% SDS) for 10 min at room temperature.

Gel Electrophoresis and Immunoblotting

Protein samples were incubated in SDS sample buffer for 10 min at 100°C before separation in a SDS-7.5% polyacrylamide gel (Laemmli, 1970). For metabolically labeled samples, the gels were dried under vacuum and exposed to x-ray film (XAR-5; Eastman Kodak, Rochester, NY) and phosphoimager screens (Molecular Dynamics, Sunnyvale, CA). The amount of labeled protein in the gels was determined directly using a laser scanning phosphor imager (model 820; Molecular Dynamics). To monitor the appearance of gp80 in the medium, aliquots of either the apical or basolateral medium were separated by SDS-PAGE under nonreducing conditions. Under these conditions, gp80 is the predominant labeled secretory protein observed in MDCK cells and migrates as a single band at approximately 80 kDa (Kondor-Koch *et al.*, 1985; Gottlieb *et al.*, 1986; Urban *et al.*, 1987).

For tubulin samples, the gels were electrophoretically transferred to Immobilon polyvinylidene fluoride membrane (Millipore, Bedford, MA). The blots were processed for enhanced chemiluminescence according to the manufactures protocol (Amersham) using a β-tubulin monoclonal antibody (Amersham). β-tubulin monoclonal antibody was visualized with a rabbit anti-mouse horseradish peroxidase-conjugated secondary antibody (Amersham).

Disruption of Microtubules with Nocodazole

Stocks of nocodazole (10 mg/ml) were prepared in dimethylsulfoxide and stored in single use aliquots at −20°C. Stock solutions of nocodazole were diluted into the appropriate medium to a final concentration of 10 μg/ml (33 μM) immediately before use. As diagrammed in the time line shown in Figure 3A, cultures were initially incubated for 30 min at 4°C in DMEM/FBS. The medium was then replace with DMEM/FBS, −met, −cys, supplemented with 33 μM nocodazole where appropriate, and the cultures were incubated for an additional 30 min at 4°C. The cultures were refed with DMEM/FBS, −met, −cys, supplemented with 33 μM nocodazole where appropriate, and shifted to 37°C for an additional 30 min. The cells were then pulse labeled as described above with the modification that 33 μM nocodazole was included in the appropriate medium. It should be noted that the microtubule organization in cultures that were exposed to 4°C treatment in the absence of nocodazole when assayed after the labeling period displayed the identical microtubule organization as cultures that had been maintained at 37°C at all time points during the development of polarity (our unpublished observations).

RESULTS

Organization of Microtubules after Establishment of Cell–Cell Contacts in MDCK Clone II/G and II/J Cells

We have analyzed two independently derived clones of MDCK cells (Gaush *et al.*, 1966; Nelson and Veshnock, 1986). Both clones form tight (TER ~250 Ωcm^2), polarized monolayers in which apical (gp80, gp135/170) and basolateral (E-cadherin) proteins are localized exclusively to specific membrane domains at steady state (Wollner *et al.*, 1992; Mays *et al.*, 1995a, 1995b).

The distribution of microtubules was examined by confocal immunofluorescence microscopy; the images are presented as stereoscopic pairs. In clone II/G cells, 24 h after induction of cell–cell adhesion, microtubules originate from a broad region of the cytoplasm near the nucleus and extend outward to the plasma membrane (Figure 1A). By 48 h, the microtubule organization in these cells had changed dramatically (Figure 1C). Microtubules form a web of filaments in the subapical membrane cytoplasm, long cortical filaments oriented parallel to the lateral membrane that span the length of the cell, and a randomly organized mat of short filaments along the basal membrane. The organization of cortical microtubules is clearest in the image of 96-h cultures in which the first 8 μm of the image stacks have been removed from the stereoscopic views (Figure 1E). The observed reorganization and final distribution of microtubules in clone II/G cells are similar to those reported previously (Bacallao *et al.*, 1989).

In direct contrast to the reorganization of microtubules in clone II/G cells, the distribution of microtubules in clone II/J cells did not change during development of cell polarity. In clone II/J cells, 24 h after the induction of cell–cell contacts, microtubules orig-

Figure 1 (facing page). Confocal images (stereoscopic pairs) of microtubules in MDCK clone II/G and II/J cells at various times after the induction of cell–cell contacts. Confluent MDCK clone II/G (A–E) and II/J (F–J) cultures were established by seeding 'contact-naive' cells at confluent density on collagen-coated polycarbonate filters in DMEM/FBS containing 5 μM Ca^{2+}. Synchronous cell–cell contact was subsequently initiated by raising the Ca^{2+} concentration of the culture medium to 1.8 mM. At the indicated times after induction of cell–cell contacts, samples were fixed and processed for immunofluorescence with monoclonal antibodies against α- and β-tubulin as described in MATERIALS AND METHODS. Stereoscopic pairs of image stacks were produced from serial images collected for each specimen using a z step of 0.2 μm. (E) The first 8 μm of the image stack were removed from the stereoscopic pairs of the 96-h sample of clone II/G cells so that the organization of cortical microtubules can be easily viewed. Bar, 10 μm.

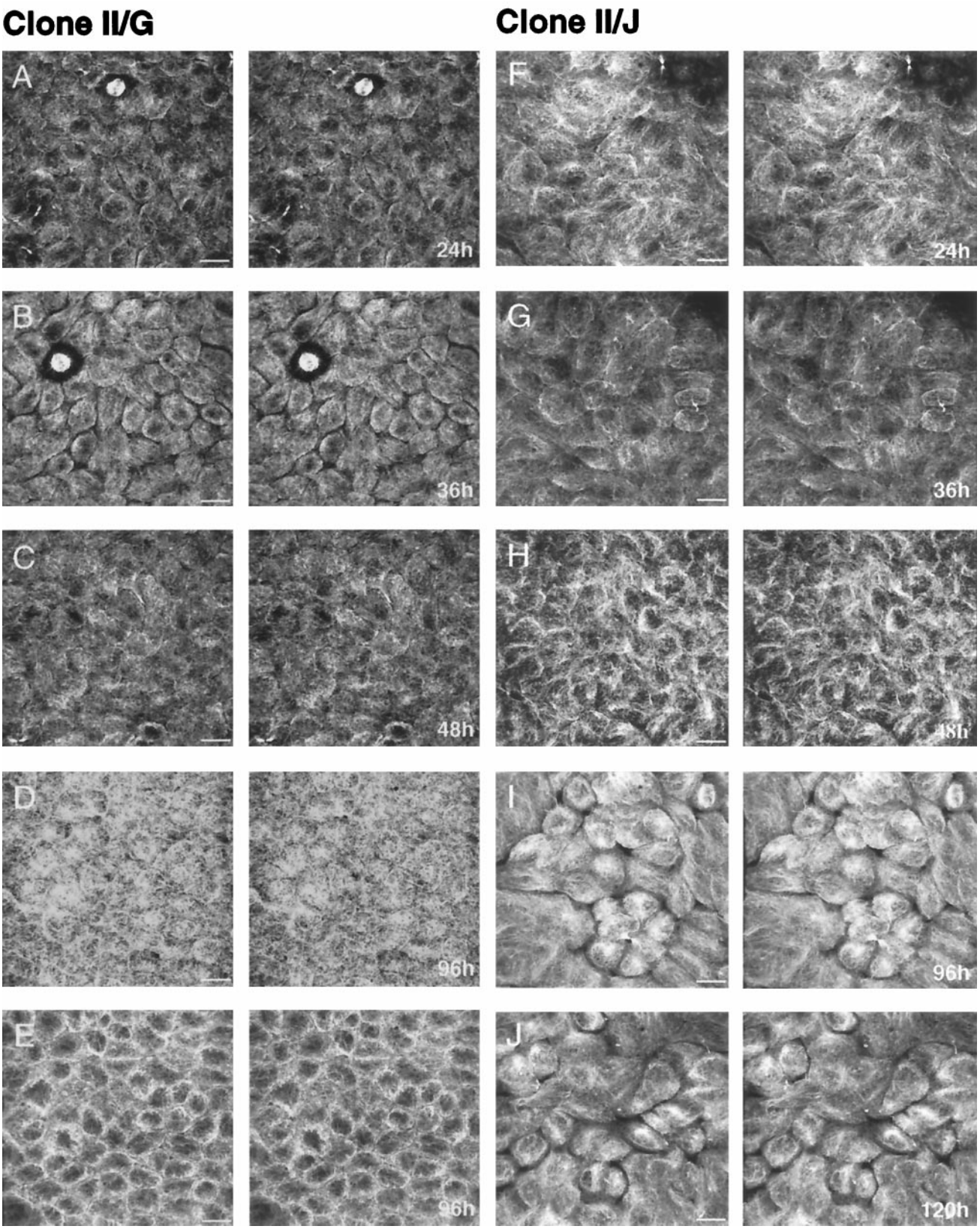
Clone II/G
Clone II/J
A
24h
F
24h
B
36h
G
36h
C
48h
H
48h
D
96h
I
96h
E
96h
J
120h

Figure 1.

inate from a broad perinuclear region of the cytoplasm and extend outward to the cell periphery (Figure 1F); this distribution is similar to that in clone II/G cells at this time (see above). However, this microtubule organization persisted in clone II/J cells maintained in culture for up to 120 h (Figure 1J).

These results show that microtubule distributions are distinctly different in two independently derived clones of MDCK cells during development of cell surface polarity. The microtubule array of nonpolarized cells from both clones is nucleated from a perinuclear site (PN-type). During the subsequent establishment of cell surface polarity, microtubules in clone II/G cells reorganize around subapical sites (AN-type), whereas those in clone II/J cells maintain a PN-type microtubule organization. Nevertheless, cells of both clones develop identical distributions of apical and basolateral membrane proteins at steady state (Wollner *et al*., 1992; Mays *et al*., 1995a, 1995b). Note that analysis of the morphology of cells from both clones at each time point revealed that on average 1) the height of clone II/J cells is 5–15% less than that of clone II/G cells; and 2) the diameter of clone II/J cells is 1.2–1.5 times greater than that of clone II/G cells (our unpublished observations).

Table 1. Localization of the Golgi complex in MDCK clone II/G and II/J cells at various times after the initiation of cell–cell contacts

	Golgi Localization	
Cell type	Perinuclear/ Circunuclear	Apiconuclear
Clone II/G		
24 h	60 ± 10	40 ± 10
36 h	26 ± 3	74 ± 3
48 h	6.2 ± 3.7	93.3 ± 4.2
96 h	0	100
120 h	0	100
Clone II/J		
24 h	75.3 ± 4.5	24.6 ± 4.5
36 h	54.5 ± 16.1	45.3 ± 20.4
48 h	79.5 ± 11.2	20.5 ± 11.6
96 h	63 ± 14.7	37 ± 14
120 h	65 ± 12.5	35 ± 12.4

Confluent MDCK clone II/G and II/J cultures were established by seeding 'contact naive' cells at confluent density on collagen-coated polycarbonate filters in DMEM/FBS containing 5 μM Ca^{2+}. Synchronous cell–cell contact was subsequently initiated by raising the Ca^{2+} concentration of the culture medium to 1.8 mM. At the indicated times after induction of cell–cell contacts, samples were fixed and stained with a monoclonal antibody against β-Cop as described in MATERIALS AND METHODS. Confocal serial images of each specimen were collected and used to determine the location of the Golgi complex with respect to the nucleus. Results for each time point are from four fields, each containing >30 cells, collected from two independent experiments (i.e., ~250 cells/time point) and are presented as the mean ± SE.

Changes in Golgi Distribution after Cell–Cell Adhesion in MDCK Clone II/G and II/J Cells

Previous studies have shown that the distribution of the Golgi complex in cells is directly related to microtubule organization (Bacallao *et al*., 1989). Therefore, we compared Golgi and microtubule distributions in clone II/G and II/J cells during development of polarity. Golgi distribution was determined by the distribution of β-COP (Allan and Kreis, 1986; Duden *et al*., 1991), which localizes to the *cis*-region of the Golgi complex; results are presented in Table 1. Twenty four hours after cell–cell adhesion, the Golgi complex in clone II/G and II/J cells was localized predominately in a perinuclear/circumnuclear position (~70% of cells). However, ~36 h after the induction of cell–cell contacts, the Golgi complex in >70% of II/G cells had relocated to an apiconuclear position, concomitant with microtubule reorganization in these cells. By 48 h, the Golgi complex in ~90% of clone II/G cells had relocalized to the apiconuclear position; after 96 h, 100% of clone II/G cells displayed this Golgi distribution. In contrast, the Golgi complex in II/J cells remained predominantly localized to the perinuclear/circumnuclear position at all time points examined (Table 1). Similar results were obtained when the Golgi was labeled with C6-NBD-ceramide (our unpublished observations). These results demonstrate an interrelationship in the distribution of microtubules and the Golgi complex; in clone II/G cells, they initially exhibit a PN-type distribution and then redistribute to an AN-type organization during development of polarity, but maintain a PN-type organization in clone II/J cells at all times.

Establishment of Direct Targeting Pathways to the Cell Surface for New Synthesized Proteins in MDCK Clone II/G and II/J Cells

That two independently derived clones of MDCK cells generate different microtubule distributions provides an opportunity to directly assess whether microtubule organization per se specifies protein targeting from the TGN to different plasma membrane domains. Furthermore, since clone II/G cells initially have a PN-type and then develop an AN-type microtubule/Golgi organization, we can examine whether protein trafficking to specific plasma membrane domains correlates temporally with transition from PN- to AN-type microtubule/Golgi organization.

We examined the direct delivery to the cell surface of three endogenous proteins. Protein delivery to either the apical or basolateral membrane domain was determined by capturing the arrival of the first wave of newly synthesized proteins at the plasma membrane. We monitored the appearance of the predominantly apical secretory protein gp80 (Kondor-Koch *et*

al., 1985; Gottlieb *et al.*, 1986; Urban *et al.*, 1987), the apical membrane protein gp135/170 (Ojakian and Schwimmer, 1988), and the basolateral membrane protein E-cadherin (Le Bivic *et al.*, 1990).

Targeting of gp80 and gp135/170 to the Apical Membrane Secretion of gp80 can be detected simply by removing medium from the apical and basolateral chambers of filter-inserts and separating proteins by nonreducing SDS-PAGE. At all times examined in both clone II/G and II/J cells, >80% of newly synthesized gp80 was secreted from the apical membrane domain (Figure 2). Arrival of gp135/170 at the plasma membrane was detected by cell surface domain-specific biotinylation; biotinylated proteins were extracted from cells and affinity isolated with a specific gp135/170 antibody followed by precipitation of biotinylated gp135/170 with avidin-agarose. Results show that, at all times examined in both II/G and II/J cells, >90% of newly synthesized gp135/170 was delivered directly to the apical membrane (Figure 2).

Targeting of E-Cadherin to the Basolateral Membrane Delivery of newly synthesized E-cadherin to the cell surface was determined by cell surface domain-specific biotinylation; biotinylated proteins were extracted from cells and affinity isolated with a specific E-cadherin antibody followed by precipitation of biotinylated E-cadherin with avidin-agarose. At all times examined in both clone II/G and II/J cells, >90% of the newly synthesized E-cadherin was targeted directly to the basolateral membrane (Figure 2).

Taken together, these results demonstrate that direct delivery pathways for gp80 and gp135/170, and E-cadherin to the apical and basolateral plasma membranes, respectively, are established in both clone II/G and II/J cells within 10 h after induction of cell–cell contacts. At this time, microtubules have a PN-type organization in both cell clones. Reorganization of microtubules to an AN-type in clone II/G cells occurs later and does not coincide with a change in the targeting of these proteins.

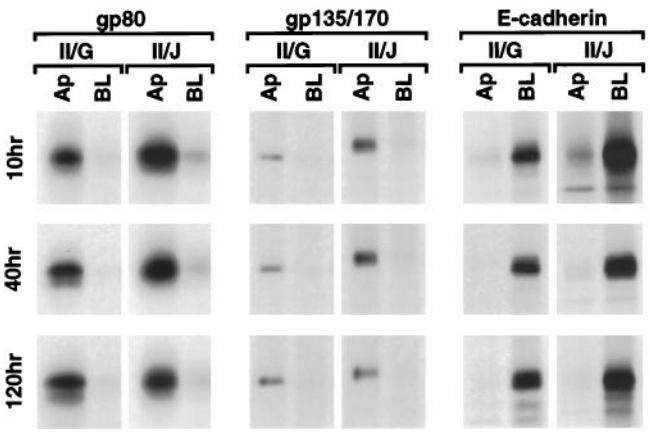

Figure 2. Targeting of newly synthesized gp80, gp135/170, and E-cadherin to the plasma membrane during the development of polarity in MDCK clone II/G and II/J cells. Confluent MDCK clone II/G and II/J cultures were established as described in MATERIALS AND METHODS. Duplicate filters from each clone were metabolically labeled with [^{35}S]methionine/cysteine for 1 h at 37°C. Immediately after the metabolic labeling period, medium was collected from the apical and basal compartments of the filter and separated by SDS-PAGE to monitor the delivery of newly synthesized gp80 to the apical (Ap) and basolateral (BL) surface. The cells were then labeled at either the apical (Ap) or basolateral (BL) surface with NHS-SS-biotin. Cells were extracted in RIPA buffer as described in MATERIALS AND METHODS. Samples were then split in half and sequentially precipitated with either a monoclonal antibody to gp135/170 or antiserum against E-cadherin followed by avidin agarose. The culture medium and immunoprecipitates from samples collected at the indicated times after the induction of cell–cell contacts were processed for SDS-PAGE and fluorography. Fluorography results from representative samples from two to four independent experiments for each time point are presented.

Role of Intact Microtubules in Protein Targeting to Cell Surface Domains in MDCK Clone II/G and II/J Cells during Development of Polarity

We next sought to examine whether intact microtubules per se are required for protein targeting irrespective of a PN- or AN-type organization. Microtubules were disrupted in MDCK clone II/G and II/J cells using a combination of cold treatment and nocodazole (Figure 3A). Microtubule breakdown was initiated by preincubating cells at 4°C followed by the addition of 33 μM nocodazole. Indirect immunofluoresence of 120-h differentiated clone II/G and II/J cells revealed no intact microtubules after nocodazole treatment (Figure 3B); identical results were observed with cells maintained in culture for shorter periods of time after the induction of cell–cell contacts (our unpublished observations). To evaluate microtubule disruption quantitatively, we examined the amount of tubulin distributed between pellet and supernatant fractions after cell extraction in microtubule-stabilizing buffer and centrifugation at 20,000 $\times$ *g* for 20 min. In extracts prepared from control cells at different stages in the development of cell polarity, >30% of tubulin was present in pellet fractions. However, after treatment with 33 μM nocodazole, tubulin was not detected in the pellet fractions, and the amount of tubulin in the supernatant fraction increased proportionally, indicating that this protocol had resulted in disruption of >99% of polymerized tubulin (Figure 3C).

We examined the effects of microtubule disruption on targeting of newly synthesized proteins to apical and basolateral membrane domains during establishment of epithelial polarity in clone II/G and II/J cells. Note that protein trafficking could still be examined by cell surface domain-specific biotinylation despite disruption of microtubules,

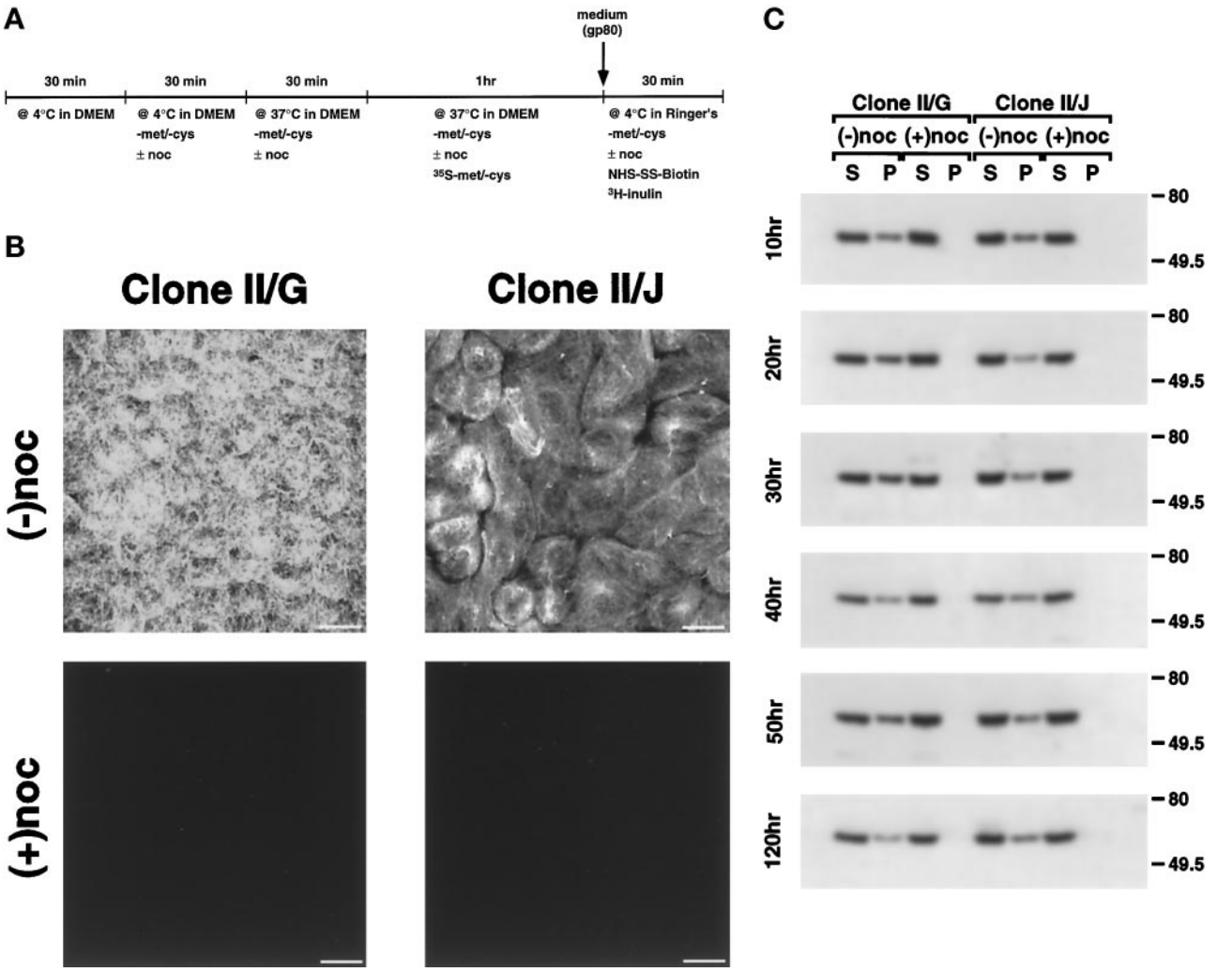

Figure 3. Distribution of tubulin in MDCK clone II/G and II/J cells after treatment with nocodazole. (A) Timeline scheme of experimental protocol used to disrupt microtubules. Confluent MDCK clone II/G and II/J cultures were established as described in MATERIALS AND METHODS. (B) After incubation in either the absence (−noc) or presence (+noc) of nocodazole, 120-h differentiated MDCK clone II/G and clone II/J cells were fixed and processed for immunofluorescence with monoclonal antibodies against α- and β-tubulin (see MATERIALS AND METHODS) to show the distribution of intact microtubules. Image stacks were produced from serial images collected for each specimen using a z step of 0.2 μm. (C) At the indicated times after the induction of cell–cell contacts, the amount of soluble (S) and polymerized tubulin (P) was determined in both clones of MDCK cells incubated in either the absence (−noc) or presence (+noc) of nocodazole. Samples were extracted in microtubule-stabilizing buffer containing 0.1% Triton X-100 and centrifuged at 20,000 × g to separate soluble (S) and insoluble fractions (P). The insoluble fractions were then solubilized in 0.5% Triton X-100. Equal amounts of supernatant and pellet fractions for each sample were separated by SDS-PAGE. Gels were then electrophoretically transferred to Immobilon polyvinylidene fluoride membrane and probed with a monoclonal antibody to β-tubulin. The β-tubulin antibody was visualized with a horseradish peroxidase-conjugated secondary antibody followed by enhanced chemiluminescence. Representative samples from two to four independent experiments for each time point are presented. Bar, 10 μm.

since tight junctions remained impermeable to the paracellular passage of inulin (our unpublished observations).

Targeting of gp80 and gp135/170 to the Apical Membrane Disruption of microtubules in II/G cells between 0 and 40 h after the induction of cell–cell contacts resulted in a ~50% decrease in apical secretion of gp80 (Figure 4A). Concomitantly, an increased proportion of gp80 was secreted into the basolateral medium. By 50 h, the inhibitory effect of microtubule disruption on apical delivery of gp80 was less pronounced, although gp80 was still missorted into the basolateral medium. Analysis of subsequent time points revealed inconsistencies between independent experiments in the amounts of gp80 secreted into the

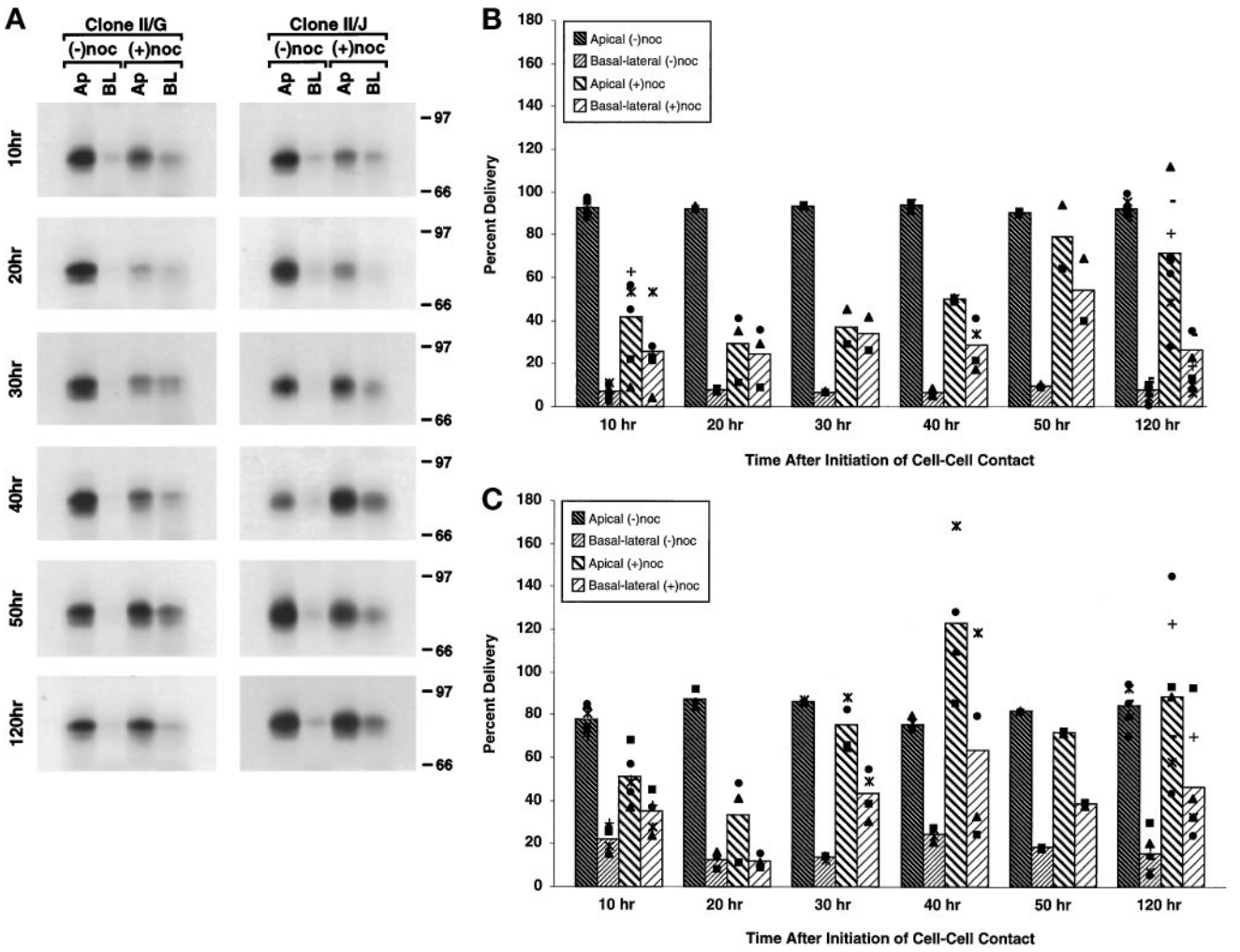

Figure 4. Role of intact microtubules in targeting of newly synthesized gp80 to the plasma membrane during the development of polarity in MDCK clone II/G and II/J cells. Confluent MDCK clone II/G and II/J cultures were established as described in MATERIALS AND METHODS. As diagrammed in Figure 3A, cultures were incubated in either the absence (−noc) or presence (+noc) of nocodazole. During the last hour at 37°C, cultures were metabolically labeled with [^{35}S]methionine/cysteine. After the metabolic labeling period, medium was collected from the apical and basal compartments of the filters. Secreted proteins were separated by SDS-PAGE to monitor the delivery of newly synthesized gp80 to the apical (Ap) and basolateral (BL) surface at the indicated times after the induction of cell–cell contacts (10–120 h). (A) Fluorography results of representative samples for each time point are presented. The amount of labeled gp80 in gels was determined directly using a Molecular Dynamics phosphor imager (model 820). Scanning densitometry results of protein from MDCK clone II/G (B) and clone II/J (C) cells are presented as a percentage of the total newly synthesized gp80 delivered to the plasma membrane in the absence of nocodazole (Percent Delivery). The bar graphs depict the mean of two to nine independent experiments, each of which is represented by one of the symbols in the scatter plots.

apical and basolateral media; results of a typical experiment are shown in Figure 4A, and the averages and individual results from eight independent experiments are presented in Figure 4B. Note that in parallel cultures of control clone II/G cells, >80% of the newly synthesized gp80 was secreted from the apical surface at all time points examined during development of cell polarity (Figure 4, A and B).

In clone II/J cells, 10 h after induction of cell–cell contacts, microtubule disruption inhibited secretion of newly synthesized gp80 into the apical medium by ~30%, with a concomitant increase in secretion of gp80 into the basolateral medium (Figure 4C). At 20 h, secretion of gp80 into the apical medium was decreased by >50% after microtubule disruption, but little or no gp80 was secreted into the basolateral medium. Thirty hours after induction of cell–cell contacts, the inhibitory effect of microtubule disruption on apical secretion of newly synthesized gp80 was markedly reduced, although significant amounts of gp80 were secreted into the basolateral medium. By 50 h, microtubule disruption did not have an inhibitory

effect on apical secretion of gp80, although we did observe pronounced variability in the amount of gp80 secreted into the basolateral medium (Figure 4C). Similar to results from clone II/G cells, we found at later times that the amounts of gp80 secreted into the apical and basolateral medium varied considerably between independent experiments (Figure 4C). Note that in control clone II/J cells, >80% of the newly synthesized gp80 was secreted into the apical medium at all times (Figure 4, A and C).

For the following reasons, we do not think that the variability in gp80 secretion into the apical and basolateral media observed at these later times is due to experimental error: 1) the effect was documented in multiple independent experiments; 2) delivery of newly synthesized gp80 in parallel control cells did not vary between individual experiments; 3) relatively little variation was detected between experiments for the other apical or basolateral membrane proteins that were prepared from the same Transwell filters in each experiment; and 4) gp80 did not diffuse between filter-insert compartments, since the tight junction remained impermeable to the paracellular diffusion of inulin after microtubule disruption. Thus, the variability between experiments likely represents the randomization of gp80 secretion from the apical and basolateral surface after disruption of microtubules. While gp80 targeting in polarized MDCK cells has previously been shown to be sensitive to microtubule disruption (Parczyk *et al.*, 1989), the changes we observed in gp80 secretion after microtubule disruption at various times after establishment of cell–cell contacts have not been reported.

After microtubule disruption in both clone II/G and II/J cells at each time examined, delivery of newly synthesized gp135/170 to the apical plasma membrane was inhibited by ~50%, but, in contrast to gp80, we did not detect a concomitant missorting of gp135/170 to the basolateral membrane. Note that >90% of newly synthesized gp135/170 was directly delivered to apical plasma membrane in control II/G and II/J cells at all times (Figure 5).

Targeting of E-Cadherin to the Basolateral Membrane

Microtubule disruption in both clone II/G and II/J cells, and at all times examined, resulted in a ~30% reduction in the amount of newly synthesized E-cadherin delivered to the basolateral plasma membrane. We did not detect any missorting of E-cadherin to the apical membrane. Note that in control clone II/G and II/J cells, >90% of newly synthesized E-cadherin was delivered directly to the basolateral plasma membrane at all times (Figure 6).

DISCUSSION

We show that direct delivery of newly synthesized gp135/170, gp80, and E-cadherin to the correct membrane domain of both clone II/G and II/J MDCK cells is established within 10 h of induction of cell–cell contacts (see also, Wollner *et al.*, 1992; Mays *et al.*, 1995b). Significantly, at this time, both clone II/G and II/J cells have a PN-type microtubule/Golgi organization; the AN-type microtubule organization did not develop in clone II/G cells until 48 h after cell–cell adhesion. Nevertheless, the PN-type of microtubule organization is important for delivery of these proteins to the cell surface; microtubule disruption in both clones of MDCK cells reduced by 25–50% the amounts of gp135/170 and E-cadherin delivered to the apical and basolateral membrane, respectively. We note that these proteins were not missorted to the incorrect membrane domain in the absence of microtubules. Delivery of gp80 to the apical membrane in newly established MDCK cultures was also decreased by ~30–50% upon microtubule disruption. In contrast to gp135/170 and E-cadherin, some missorting of gp80 to the basolateral membrane was detected in the absence of microtubules. In fully differentiated cells treated with nocodazole, gp80 delivery to both membrane domains was variable and nonspecific. Thus, gp80 represents a class of apical proteins that requires intact microtubules for efficient and appropriate delivery to the cell surface.

We draw two conclusions from these results. First, intact microtubules appear to facilitate the delivery of proteins to both the apical and basolateral plasma membranes. This result confirms a role for microtubules in facilitating protein delivery to the apical membrane (Rindler *et al.*, 1987; Achler *et al.*, 1989; Eilers *et al.*, 1989; Matter *et al.*, 1990; van Zeijl and Matlin, 1990; Gilbert *et al.*, 1991). In contrast to several previous studies (Rindler *et al.*, 1987; Achler *et al.*, 1989; Eilers *et al.*, 1989; Matter *et al.*, 1990; van Zeijl and Matlin, 1990), our results show that microtubules are also required to facilitate targeting of membrane proteins to the basolateral membrane. The reason for this discrepancy is not easily reconciled. We note that >99% of microtubules were disrupted in our experiments. In addition, our labeling protocol was designed to capture the initial wave of protein reaching the plasma membrane and, therefore, we cannot comment on the effects of microtubule disruption on the kinetics of protein delivery at later chase times (see Gilbert *et al.*, 1991).

Second, direct delivery of proteins to the cell surface is independent of a specific microtubule organization. Our results show unequivocally that the AN-type microtubule/Golgi organization does not represent a specialized structural framework in epithelial cells for vesicle targeting from the TGN to either the apical or basolateral membrane. Thus, either the polarity of microtubules between the TGN and different membrane domains is not important with respect to vesicle trafficking in cells with PN- and AN-type organizations,

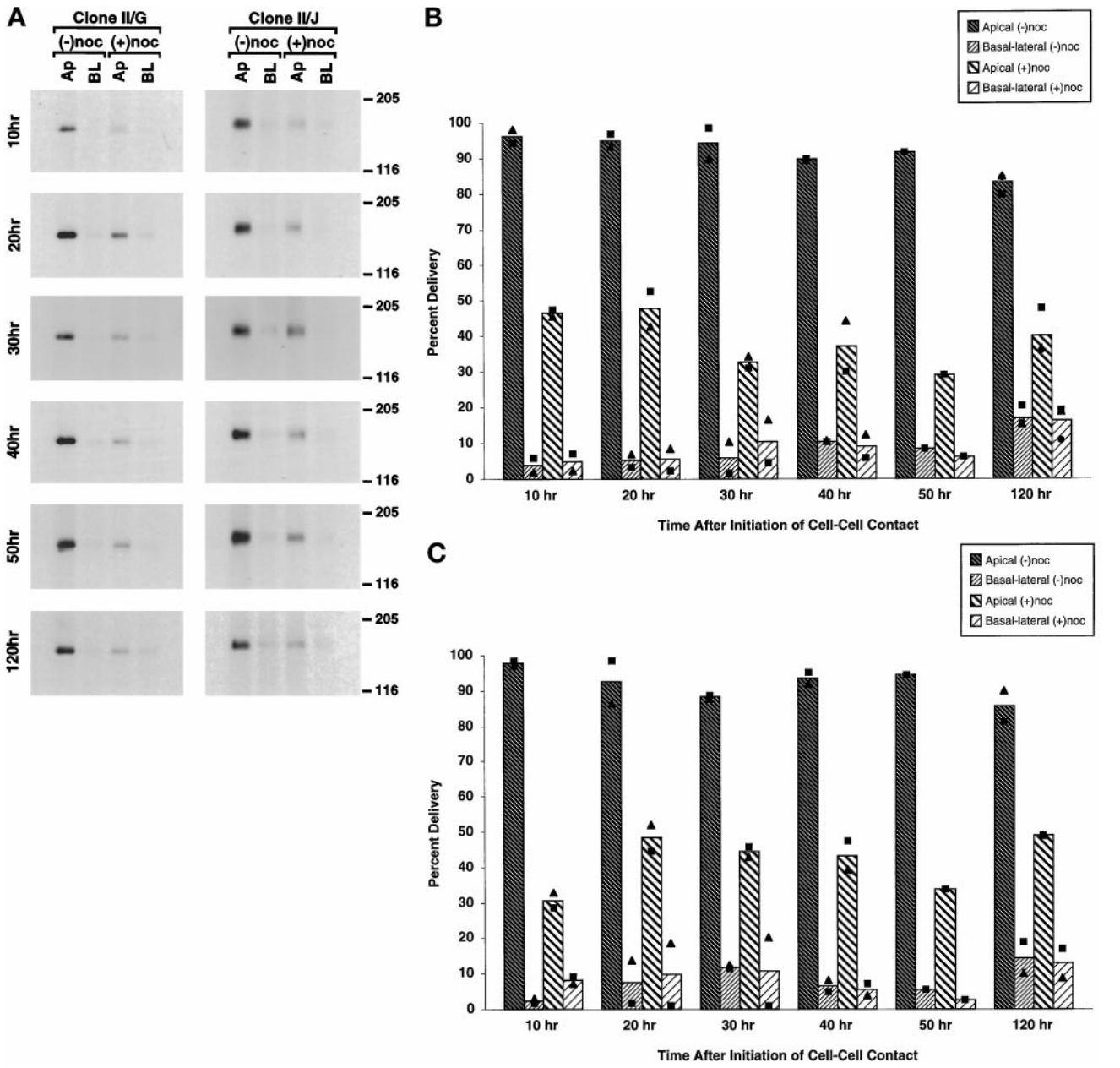

Figure 5. Role of intact microtubules in targeting of newly synthesized gp135/170 to the plasma membrane during the development of polarity in MDCK clone II/G and II/J cells. Confluent MDCK clone II/G and II/J cultures were established as described in MATERIALS AND METHODS. As diagrammed in Figure 3A, cultures were incubated in either the absence (−noc) or presence (+noc) of nocodazole. During the last hour at 37°C, cultures were metabolically labeled with [^{35}S]methionine/cysteine. At the indicated times after the induction of cell–cell contacts (10–120 h), duplicate filters were labeled on either the apical (Ap) or basolateral (BL) membrane with NHS-SS-biotin. Cells were than extracted in RIPA buffer as described in MATERIALS AND METHODS. Samples were sequentially precipitated with a monoclonal antibody to gp135/170 followed by avidin agarose. Immunoprecipitates were then processed for SDS-PAGE and fluorography. (A) Fluorography results from representative samples for each time point are presented. The amount of labeled gp135/170 in gels was determined directly using a Molecular Dynamics phosphor imager (model 820). Scanning densitometry results of protein from MDCK clone II/G (B) and clone II/J (C) cells are presented as a percentage of the total newly synthesized gp135/170 delivered to the plasma membrane in the absence of nocodazole (Percent Delivery). The bar graphs depict the mean of one to three independent experiments, each of which are represented by one of the symbols in the scatter plots.

or vesicles can adapt to different microtubule orientations due to the presence on their membrane of plus- and minus-end–directed microtubule motors. Lafont *et al.* (1994) have presented evidence that in polarized

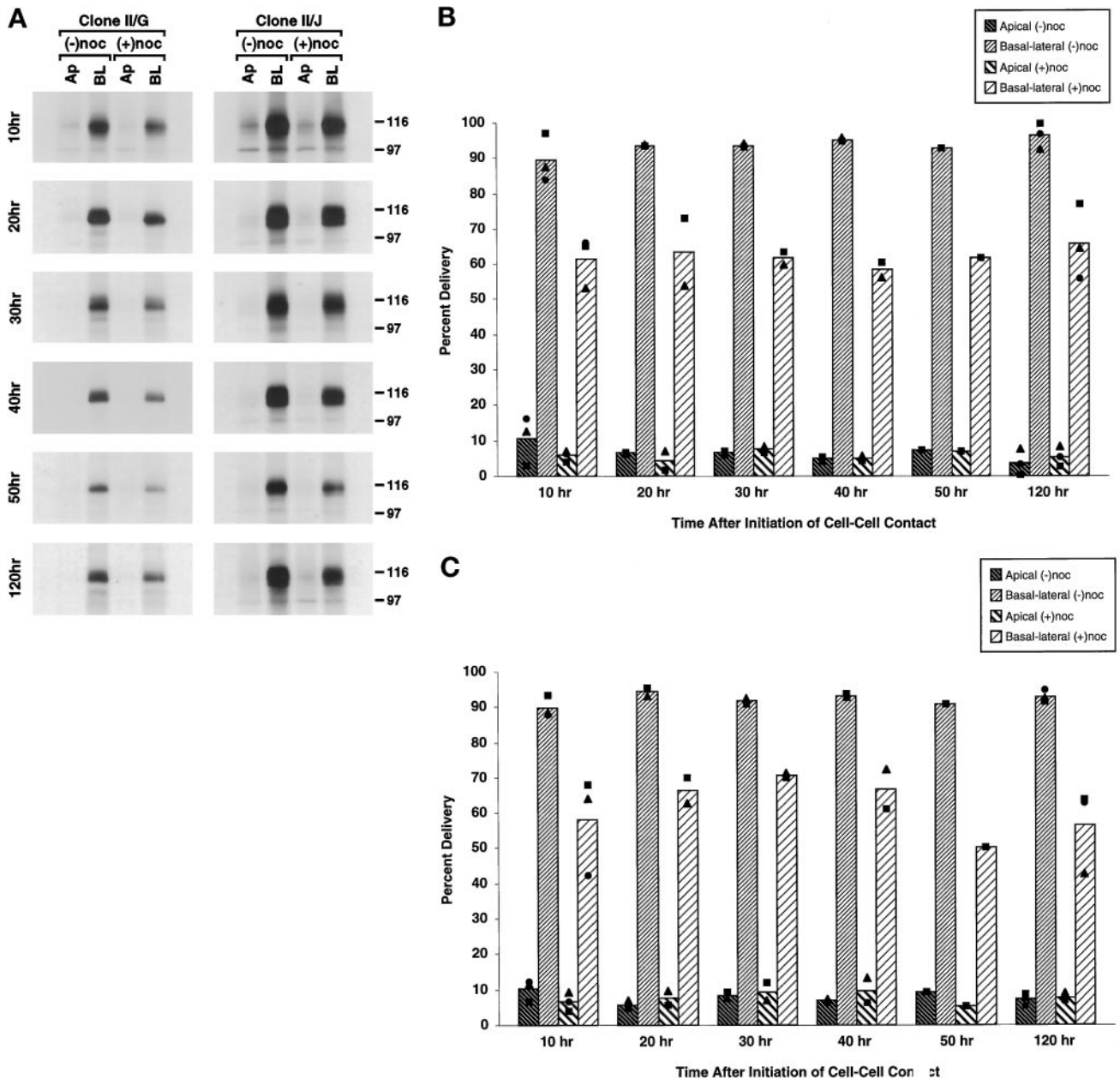

Figure 6. Role of intact microtubules in the targeting of newly synthesized E-cadherin to the plasma membrane during the development of polarity in MDCK clone II/G and II/J cells. Confluent MDCK clone II/G and II/J cultures were established as described in MATERIALS AND METHODS. As diagrammed in Figure 3A, cultures were incubated in either the absence (−noc) or presence (+noc) of nocodazole. During the last hour at 37°C, cultures were metabolically labeled with [^{35}S]methionine/cysteine. At the indicated times after the induction of cell–cell contacts (10–120 h), duplicate filters were labeled on either the apical (Ap) or basolateral (BL) membrane with NHS-SS-biotin. Cells were than extracted in RIPA buffer as described in MATERIALS AND METHODS. Samples were sequentially precipitated with an antiserum to E-cadherin followed by avidin agarose. Immunoprecipitates were then processed for SDS-PAGE and fluorography. (A) Fluorography results from representative samples for each time point are presented. The amount of labeled E-cadherin in gels was determined directly using a Molecular Dynamics phosphor imager (model 820). Scanning densitometry results of protein from MDCK clone II/G (B) and clone II/J (C) cells are presented as a percentage of the total newly synthesized E-cadherin delivered to the plasma membrane in the absence of nocodazole (Percent Delivery). The bar graphs depict the mean of one to three independent experiments, which are represented by one of the symbols in the scatter plots.

MDCK cells, both plus-end (kinesin)- and minus-end (dynein)–directed microtubule motors are involved in transport of hemagglutinin to the apical membrane, whereas only a plus-end–directed motor (kinesin) is

involved in transport of VSV G protein to the basolateral membrane. Delivery of gp80-containing vesicles to the apical (and basolateral) membrane in cells with a PN-type microtubule organization is toward the plus-ends of microtubules, whereas apical delivery of gp80-containing vesicles in cells with a AN-type organization would require a minus-end–directed motor. Therefore, it is likely that gp80 vesicles contain both plus- and minus-end–directed motors. However, it unclear at this time how cells ensure that gp80-containing vesicles are delivered predominantly along microtubules that extend toward the apical plasma membrane in PN-type cells. In cells with an AN-type microtubule organization, it is possible that either the plus-end–directed motor becomes less active or the minus-end–directed motor becomes dominant in determining the direction of vesicle movement; this transition would presumably not occur in clone II/J cells as they differentiate. As with gp80, gp135/170-containing vesicles must also contain both plus- and minus-end–directed motors. We note, however, that gp135/170 was never missorted to the basolateral membrane under control conditions or after disruption of microtubules. E-cadherin, which was never missorted to the apical membrane, would only require a plus-end–directed motor for appropriate delivery to the basolateral membrane in cells with either a PN- or AN-type microtubule organization.

Our previous studies showed that an increasing proportion of αNa/K-ATPase is delivered directly to the basolateral membrane in II/G cells coincident with the development of an AN-type microtubule/Golgi organization; αNa/K-ATPase delivery in II/J cells remained ~50:50 to both membrane domains (Mays *et al.*, 1995b). However, sorting of αNa/K-ATPase, but not E-cadherin, to the basolateral membrane in II/G cells appeared to depend on glycosphingolipid (GSL) sorting, which excluded αNa/K-ATPase from the apical pathway. Inhibition of GSL synthesis in II/G cells with fumonisin resulted in delivery of αNa/K-ATPase equally to the apical and basolateral membranes, as in II/J cells, without any affect on E-cadherin sorting (Mays *et al.*, 1995b). However, as with E-cadherin, there is little or no affect of microtubule disruption on missorting of αNa/K-ATPase to the apical membrane (i.e., the amount of αNa/K-ATPase delivered to the apical membrane is not altered in the presence of nocodazole; Grindstaff and Nelson, unpublished results; see also Boll *et al.*, 1991). Furthermore, treatment of II/G cells with fumonisin does not affect gp80 and E-cadherin sorting (Mays *et al.*, 1995b), whereas microtubule disruption produces a marked reduction in the delivery of these proteins to their appropriate membrane domains. We conclude that the effects of GSLs on sorting of αNa/K-ATPase in the TGN are distinct from the role of microtubules in delivery of transport vesicles between the TGN and plasma membrane domains.

The rapid establishment of efficient and specific targeting of proteins to the apical and basolateral membrane indicates that protein-sorting pathways develop quickly after induction of cell–cell contacts. Previous studies have shown that the cell surface distribution of apical proteins, including gp135/170, is polarized in single MDCK cells attached to a substratum (Vega-Salas *et al.*, 1987; Ojakian and Schwimmer, 1988). Basolateral membrane proteins, on the other hand, are randomly distributed on both the free (apical) surface and the basal membrane of single cells (Nelson and Veshnock, 1986; Vega-Salas *et al.*, 1987; Salas *et al.*, 1988). These results suggest that cell surface polarity of basolateral proteins requires induction of cadherin-based cell–cell adhesion. Because sorting of apical and basolateral membrane proteins into discrete transport vesicles occurs in 'nonpolarized' fibroblasts (Musch *et al.*, 1996; Yoshimori *et al.*, 1996), it is likely that sorting of apical and basolateral proteins occurs constitutively in MDCK cells, regardless of the state of cell–substratum or cell–cell adhesion.

If all cell surface proteins were sorted in the TGN into a single class of apical or basolateral transport vesicles, we would expect that gp80 would exhibit characteristics of gp135/170 delivery. Similar to gp135/170, gp80 was delivered directly to the apical membrane domain within 10 h of induction of cell–cell contacts. Microtubule disruption resulted initially in a 30–50% reduction in delivery of gp80 to the apical membrane, similar to gp135/170. However, in contrast to gp135/170, a significant amount of gp80 was missorted to the basolateral membrane domain. Our results indicate that vesicles containing gp80 require intact microtubules to specify their delivery to the apical membrane, and that, in the absence of microtubules, these vesicles are able to dock and fuse with the basolateral membrane. Similar results have been reported for the targeting of basement proteins in MDCK cells and LLC-PK_1 renal epithelial cells and serum albumin in rat hepatocytes after microtubule disruption (Boll *et al.*, 1991; De Almeida and Stow, 1991; Saucan and Palade, 1991). This suggests that gp80 represents a class of proteins that is sorted into a population of vesicles that have promiscuous docking capabilities with both membrane domains. In contrast, gp135/170 and E-cadherin represent two additional classes of proteins whose specificity of delivery is primarily dependent on membrane domain-specific organization of docking and fusion machinery, rather than establishment of microtubule-based targeting pathways.

In summary, we have shown that redistribution of microtubules and the Golgi complex from a PN-type organization characteristic of 'nonpolarized' cells to an AN-type organization is not required to establish

direct delivery pathways from the TGN to either the apical or basolateral membrane domain. Thus, the fidelity of post-TGN transport vesicle delivery to the correct membrane domain appears to be determined by domain-specific vesicle-docking machinery.

ACKNOWLEDGMENTS

This work was supported by a grant from the National Institutes of Health to W.J.N. (GM35527) and a Digestive Disease Center Pilot/Feasibility study grant to K.K.G. K.K.G. was also supported by a Cancer Biology grant awarded to Stanford University from the National Cancer Institute (CA09302) and is a recipient of a postdoctoral fellowship from the National Institutes of Health.

REFERENCES

Achler, C., Filmer, D., Merte, C., and Drenckhahn, D. (1989). Role of microtubules in polarized delivery of apical membrane proteins to the brush border of the intestinal epithelium. J. Cell Biol. *109*, 179–189.

Allan, V.J., and Kreis, T.E. (1986). A microtubule-binding protein associated with membranes of the Golgi apparatus. J. Cell Biol. *103*, 2229–2239.

Bacallao, R., Antony, C., Dotti, C., Karsenti, E., Stelzer, E.H.K., and Simons, K. (1989). The subcellular organization of Madin-Darby Canine Kidney cells during the formation of a polarized epithelium. J. Cell Biol. *109*, 2817–2832.

Boll, W., Partin, J.S., Katz, A.I., Caplan, M.J., and Jamieson, J.D. (1991). Distinct pathways for basolateral targeting of membrane and secretory proteins in polarized epithelial cells. Proc. Natl. Acad. Sci. USA *88*, 8592–8596.

De Almeida, J.B., and Stow, J.L. (1991). Disruption of microtubules alters polarity of basement membrane proteoglycan secretion in epithelial cells. Am. J. Physiol. *260*, C691–700.

Duden, R., Griffiths, G., Frank, R., Argos, P., and Kreis, T.E. (1991). Beta-COP, a 110 kd protein associated with non-clathrin-coated vesicles and the Golgi complex, shows homology to beta-Adaptin. Cell *64*, 649–665.

Eilers, U., Klumperman, J., and Hauri, H.P. (1989). Nocodazole, a microtubule-active drug, interferes with apical protein delivery in cultured intestinal epithelial cells (Caco-2). J. Cell Biol. *108*, 13–22.

Fath, K.R., and Burgess, D.R. (1993). Golgi-derived vesicles from developing epithelial cells bind actin filaments and possess myosin-I as a cytoplasmically orientated peripheral membrane protein. J. Cell Biol. *120*, 117–127.

Gaush, C.R., Hard, W.L., and Smith, T.F. (1966). characterization of an established line of canine kidney cells (MDCK). Proc. Soc. Exp. Biol. Med. *122*, 931–935.

Gilbert, T., Le Bivic, A., Quaroni, A., and Rodriguez-Boulan, E. (1991). Microtubular organization and its involvement in the biogenetic pathways of plasma membrane proteins in Caco-2 intestinal epithelial cells. J. Cell Biol. *113*, 275–288.

Gottlieb, T.A., Baudry, G., Rizzolo, L., Colman, A., Rindler, M., Adesnik, M., and Sabatini, D.D. (1986). Secretion of endogenous and exogenous proteins from polarized MDCK cell monolayers. Proc. Natl. Acad. Sci. USA *83*, 2100–2104.

Hammerton, R.W., Krzeminski, K.A., Mays, R.W., Ryan, T.A., Wollner, D.A., and Nelson, W.J. (1991). Mechanism for regulating cell surface distribution of Na+, K+-ATPase in polarized epithelial cells. Science *254*, 847–850.

Hinck, L., Näthke, I.S., Papkoff, J., and Nelson, W.J. (1994). Dynamics of cadherin/catenin complex formation: novel protein interactions and pathways of complex assembly. J. Cell Biol. *125*, 1327–1340.

Kondor-Koch, C., Bravo, R., Fuller, S.D., Cutler, D., and Garoff, H. (1985). Exocytic pathways exist to both the apical and the basolateral cell surface of the polarized epithelial cell MDCK. Cell *43*, 297–306.

Laemmli, U.K. (1970). Cleavage of structural proteins during the assembly of the head of bacteriophage T4. Nature *227*, 683–685.

Lafont, F., Burkhardt, J., and Simons, K. (1994). Involvement of microtubule motors in basolateral and apical transport in kidney cells. Nature *372*, 801–803.

Le Bivic, A., Sambuy, Y., Mostov, K., and Rodriguez-Boulan, E. (1990). Vectorial targeting of an endogenous apical membrane sialoglycoprotein and uvomorulin in MDCK cells. J. Cell Biol. *110*, 1533–1539.

Louvard, D. (1980). Apical membrane aminopeptidase appears at site of cell-cell contact in cultured kidney epithelial cells. Proc. Natl. Acad. Sci. USA *77*, 4132–4136.

Marrs, J.A., Napolitano, E.W., Murphy-Erdosh, C., Mays, R.W., Reichardt, L.F., and Nelson, W.J. (1993). Distinguishing roles of the membrane-cytoskeleton and cadherin mediated cell-cell adhesion in generating different Na+, K(+)-ATPase distributions in polarized epithelia. J. Cell Biol. *123*, 149–64.

Matter, K., Bucher, K., and Hauri, H.P. (1990). Microtubule perturbation retards both the direct and the indirect apical pathway but does not affect sorting of plasma membrane proteins in intestinal epithelial cells (Caco-2). EMBO J. *9*, 3163–3170.

Matter, K., and Mellman, I. (1994). Mechanisms of cell polarity: sorting and transport in epithelial cells. Curr. Opin. Cell Biol. *6*, 545–554.

Mays, R.W., Beck, K.A., and Nelson, W.J. (1994). Organization and function of the cytoskeleton in polarized epithelial cells: a component of the protein sorting machinery. Curr. Opin. Cell Biol. *6*, 16–24.

Mays, R.W., Nelson, W.J., and Marrs, J.A. (1995a). Generation of epithelial cell polarity: Roles for protein trafficking, membrane-cytoskeleton, and E-cadherin mediated cell adhesion. Cold Spring Harbor Symp. Quant. Biol. *60*, 763–773.

Mays, R.W., Siemers, K.A., Fritz, B.A., Lowe, A.W., van Meer, G., and Nelson, W.J. (1995b). Hierarchy of mechanisms involved in generating Na/K-ATPase polarity in MDCK epithelial cells. J. Cell Biol. *130*, 1105–1115.

Musch, A., Xu, H., Shields, D., and Rodriguez-Boulan, E. (1996). Transport of vesicular stomatitis virus G protein to the cell surface is signal mediated in polarized and nonpolarized cells. J. Cell Biol. *133*, 543–558.

Nelson, W.J. (1991). Cytoskeleton functions in membrane traffic in polarized epithelial cells. Semin. Cell Biol. *2*, 375–385.

Nelson, W.J., and Veshnock, P.J. (1986). Dynamics of membrane-skeleton (fodrin) organization during development of polarity in Madin-Darby canine kidney epithelial cells. J. Cell Biol. *103*, 1751–1765.

Nelson, W.J., and Veshnock, P.J. (1987). Modulation of fodrin (membrane skeleton) stability by cell-cell contact in Madin-Darby canine kidney epithelial cells. J. Cell Biol. *104*, 1527–1537.

Ojakian, G.K., and Schwimmer, R. (1988). The polarized distribution of an apical cell surface glycoprotein is maintained by interactions with the cytoskeleton of madin-darby canine kidney cells. J. Cell Biol. *107*, 2377–2378.

Ojakian, G.K., and Schwimmer, R. (1992). Antimicrotubule drugs inhibit the polarized insertion of an intracellular glycoprotein pool

into the apical membrane of Madin-Darby canine kidney (MDCK) cells. J. Cell Sci. *103*, 677–687.

Parczyk, K., Haase, W., and Kondor-Koch, C. (1989). Microtubules are involved in the secretion of proteins at the apical cell surface of the polarized epithelial cell, Madin-Darby Canine Kidney. J. Biol. Chem. *264*, 16837–16846.

Rindler, M.J., Ivanov, I.E., and Sabatini, D.D. (1987). Microtubule-acting drugs lead to the nonpolarized delivery of the influenza hemagglutinin to the cell surface of polarized Madin-Darby canine kidney cells. J. Cell Biol. *104*, 231–241.

Rodriguez-Boulan, E., and Nelson, W.J. (1989). Morphogenesis of the polarized epithelial cell phenotype. Science *245*, 718–725.

Salas, P.J., Misek, D.E., Vega Salas, D.E., Gundersen, D., Cereijido, M., and Rodriguez-Boulan, E. (1986). Microtubules and actin filaments are not critically involved in the biogenesis of epithelial cell surface polarity. J. Cell Biol. *102*, 1853–1867.

Salas, P.J.I., Vega-Salas, D., Hochman, J., Rodriguez-Boulan, E., and Edidin, M. (1988). Selective anchoring in the specific plasma membrane domain: a role in epithelial cell polarity. J. Cell Biol. *107*, 2363–2376.

Saucan, L., and Palade, G.E. (1991). Differential colchicine effects on the transport of membrane and secretory proteins in rat hepatocytes in vivo: bipolar secretion of albumin. Hepatology *15*, 714–721.

Siemers, K.A., Wilson, R., Mays, R.W., Ryan, T.A., Wollner, D.A., and Nelson, W.J. (1993). Delivery of Na+ K+ -ATPase in polarized epithelial cells. Science *260*, 554–556.

Urban, J., Parczyk, K., Leutz, A., Kayne, M., and Kondor-Koch, C. (1987). Constitutive apical secretion of an 80-kD sulfated glycoprotein complex in the polarized epithelial Madin-Darby canine kidney cell line. J. Cell Biol. *105*, 2735–2743.

Van der Sluijs, P., Bennett, M.K., Antony, C., Simons, K., and Kreis, T.E. (1990). Binding of exocytic vesicles from MDCK cells to microtubules in vitro. J. Cell Sci. *95*, 545–553.

van Zeijl, M.J.A.H., and Matlin, K. S. (1990). Microtubule perturbation inhibits intracellular transport of an apical membrane glycoprotein in a substrate-dependent manner in polarized Madin-Darby canine kidney epithelial cells. Cell Regul. *1*, 921–936.

Vega-Salas, D.E., Salas, P.J., Gundersen, D., and Rodriguez-Boulan, E. (1987). Formation of the apical pole of epithelial (Madin-Darby canine kidney) cells: polarity of an apical protein is independent of tight junctions while segregation of a basolateral marker requires cell-cell interactions. J. Cell Biol. *104*, 905–916.

Wandinger-Ness, A., Bennett, M.K., Antony, C., and Simons, K. (1990). Distinct transport vesicles mediate the delivery of plasma membrane proteins to the apical and basolateral domains of MDCK cells. J. Cell Biol. *111*, 987–1000.

Wollner, D.A., Krzeminski, K.A., and Nelson, W.J. (1992). Remodeling the cell surface distribution of membrane proteins during the development of epithelial cell polarity. J. Cell Biol. *116*, 889–899.

Yoshimori, T., Keller, P., Roth, M.G., and Simons, K. (1996). Different biosynthetic transport routes to the plasma membrane in BHK and CHO cells. J. Cell Biol. *133*, 247–256.